Coupled Multi-Dimensional Models for Shape Memory Alloy Nanostructures: Microstructure Evolution in Nanofilms

Dhote, R., Melnik, R., Gomez, H., Sebetci, A., and Zu, J.

In: Proceedings of 6WCSCM Sixth World Conference on Structural Control and Monitoring, 15-17 July, 2014, Barcelona, Spain, J. Rodellar, A. Guemes, and F. Pozo (Eds.), Paper 445 (5 pages), pp. 2140 - 2144, CIMNE, ISBN 978-84-942844-5-8.

6WCSCM

Sixth World Conference on Structural Control and Monitoring

Barcelona, Spain, 15 - 17 July 2014

J. Rodellar, A. Güemes and F. Pozo (Eds.)

Sixth World Conference on Structural Control and Monitoring

Proceedings of the 6th edition of the World Conference of the International Association for Structural Control and Monitoring (IACSM), held in Barcelona, Spain

15-17 July 2014

Edited by:

J. Rodellar
Universitat Politècnica de Catalunya-BarcelonaTech, Spain

A. Güemes
Universidad Politécnica de Madrid, Spain

F. Pozo
Universitat Politècnica de Catalunya-BarcelonaTech, Spain

A publication of:

International Center for Numerical Methods in Engineering (CIMNE)
Barcelona, Spain

Sixth World Conference on Structural Control and Monitoring
J. Rodellar, A. Güemes, F. Pozo (Eds.)

First edition, July 2014

Printed by: Artes Gráficas Torres, S.A., Huelva 9, 08940 Cornellà de Llobregat, Spain

E-book
Depósito legal: B-16311-2014
ISBN: 978-84-942844-6-5

PREFACE

This Ebook contains the full papers of the works presented at the Sixth World Conference on Structural Control and Monitoring, 6WCSCM, Barcelona, Spain, July 15-17, 2014

6WCSCM is the 6th edition of the World Conference of the International Association for Structural Control and Monitoring (IACSM), hosted by the Universitat Politècnica de Catalunya-BarcelonaTech (UPC) under the auspices of the European Association for the Control of Structures (EACS).

The WCSCM is a premier leading conference devoted to the theoretical, numerical, experimental and practical advancements of monitoring and control technologies for dynamic structures in a wide range of civil, infrastructure, mechanical, aerospace and energy systems. This new edition will have gathered an international community contributing to the state of the art in such multidisciplinary scientific and engineering environment with new results, fresh ideas and future perspectives.

Previous editions of the conference were held in Pasadena - USA (1994), Kyoto - Japan (1998), Como - Italy (2002), La Jolla - USA (2006) and Tokyo - Japan (2010), with an increasing number of participants in each edition. 6WCSCM has attracted over 375 participants, coming from all over the world. All together around 400 lectures will have been presented, including 6 plenary lectures, which reflect the current state of the research and advances in the field.

The organizers would like to thank the authors for submitting their contributions and for their respect of the deadlines. Special thanks go to the colleagues who contributed to the organization of the 21 Special Sessions.

Barcelona (Spain) is a perfect environment for the 6WCSCM, being one of the most charming cities along the Mediterranean coast, which always offers the perfect environment for unforgettable events and plenty of enjoyable social, cultural and touristic opportunities.

In the name of the institutions and the human teams involved in the organization, we warmly hope the participants will have enjoyed the conference and the city. We also hope these proceedings will be a valuable open source of information and ideas for the future.

José Rodellar

Univ. Politècnica
de Catalunya
Barcelona, Spain

Alfredo Güemes

Univ. Politécnica de
Madrid,
Madrid, Spain

Francesc Pozo

Univ. Politècnica
de Catalunya
Barcelona, Spain

Coupled Multi-dimensional Models for Shape Memory Alloy Nanostructures: Microstructure Evolution in Nanofilms

Rakesh Dhote[1,3], Hector Gomez[2], Roderick Melnik[3], Ali Sebetci[4], and Jean Zu[1]

Abstract

We provide details of a new model and its numerical implementation, based on the isogeometric analysis, describing the dynamics of shape memory alloys in multi-dimensional cases. The core of the model is given by the phase-field equations that can capture complex thermo-mechanical behaviors of systems at different scales, including maartenstic transformations. The model is based on Ginzburg-Landau theory and requires a non-convex free energy function for an adequate description of these materials. While other examples are mentioned, main exemplifications of numerical simulations, presented here, are given for nanofilms.

I. INTRODUCTION

Shape memory alloys (SMAs) are used extensively in structural control and monitoring, in particular as parts of micro- and nano- actuators and sensors [1]. These applications require the analysis of corresponding structures with increasingly diverse geometries at various spatial scales. This leads to the importance of developing general multi-dimensional models for SMAs, in particular in dynamic situations.

Different modelling approaches have been applied for the description of dynamic behaviours of SMAs. Among them, we mention (a) the kinetic model using independent order parameter(s) (OPs) and (b) the strain-based OP PF models. In this contribution, we will focus on the latter approach. While this approach has a number of advantages, it leads to serious numerical challenges, as one has to deal with higher order spatial derivatives in this case. Furthermore, multi-dimensional models describing SMAs in full dynamic, rather than quasi-static, settings have to be developed.

The full 3D dynamic model in its generality for dynamic shape memory alloy studies was first formulated in [2]. More recently, efficient numerical implementations have been developed to achieve geometrical flexibility, focusing specifically on the strain-based OP phase-field modelling approach mentioned above. The method of choice has been the Isogeometric Analysis (IGA) methodology [3]. It has been originally developed to avoid mesh generation difficulties during engineering analysis by using non-uniform rational B-splines (NURBS) as basis functions. The use of rich basis functions provides IGA with a unique capability to model geometry exactly, in many instances, while field variables can be approximated with enhanced accuracy as it was demonstrated in a number of different applications. However, in the context of SMAs, the development and application of the IGA methodology is of very recent origin [6].

Given the current importance and an increasing range of applications of shape memory alloy nanofilms [1], [4], [5], our main exemplifications here will be given for this type of nanostructures. Our starting point is the coupled equations of nonlinear thermoelasticity, developed using the PF model and the Ginzburg-Landau theory. They are presented in Section II. These equations are discussed in the IGA framework by using a variational formulation, and the details of the numerical implementation of the SMA governing equations in the IGA framework are given in Section III. The developed methodology is exemplified in Section IV with numerical simulations on nanostructured SMA film domains subjected to different loads. Conclusions are given in Section V.

II. DYNAMICS OF SHAPE MEMORY ALLOYS

We focus here on cubic-to-tetragonal phase transformations typical in such SMA alloys as NiAl, FePd, InTl, and many others. The main part of the model to describe the dynamics of these materials can be readily obtained. In what follows, our unknowns are the displacement field $\boldsymbol{u} = \{u_1, u_2, u_3\}^T$ and the temperature θ, considered in the physical domain $\Omega \subset \mathbb{R}^3$ (an open set parameterized by Cartesian coordinates $\boldsymbol{x} = \{x_1, x_2, x_3\}^T$). We use the Cauchy-Lagrange strain tensor $\boldsymbol{\epsilon} = \{\epsilon_{ij}\}$, whose components are defined as $\epsilon_{ij} = (u_{i,j} + u_{j,i})/2$, $i, j \in$

*This work was supported by NSERC and CRC Program, TUBITAK, and ERC

[1]Rakesh Dhote is with Mechanical and Industrial Engineering, University of Toronto, 5 King's College Road, Toronto, ON, M5S3G8, Canada and with the M^{2}NeT Laboratory, Wilfrid Laurier University, Waterloo, ON,N2L3C5, Canada

[2]Hector Gomez is with the Department of Applied Mathematics, University of A Coruña Campus de Elvina, s/n. 15192 A Coruña, Spain

[3]Roderick Melnik is with the M^{2}NeT Laboratory, Wilfrid Laurier University, Waterloo, ON,N2L3C5, Canada (corresponding author: +1-519-884-1970, ext. 3662) rmelnik@wlu.ca

[4]Ali Sebetci is with the Department of Mechanical Engineering, Mevlana University, 42003, Konya, Turkey

$\{1, 2, 3\}$, where an inferior comma denotes partial differentiation (e.g., $u_{i,j} = \partial u_i/\partial x_j$). Our notations are standard and we follow [7] in the description of main parts of the model applied for our problem here. Using the strain tensor, we define the strain measures e_i, for $i = 1, \ldots, 6$ as follows:

$$\begin{Bmatrix} e_1 \\ e_2 \\ e_3 \\ e_4 \\ e_5 \\ e_6 \end{Bmatrix} = \left[\begin{array}{c|c} \mathbb{D}_3 & \mathbb{O}_3 \\ \hline \mathbb{O}_3 & \mathbb{I}_3 \end{array}\right] \begin{Bmatrix} \epsilon_{11} \\ \epsilon_{22} \\ \epsilon_{33} \\ \epsilon_{23} \\ \epsilon_{13} \\ \epsilon_{12} \end{Bmatrix}, \tag{1}$$

where $\mathbb{D}_3$, $\mathbb{O}_3$, $\mathbb{I}_3$ are 3×3 constant matrices. In particular,

$$\mathbb{D}_3 = \begin{bmatrix} 1/\sqrt{3} & 1/\sqrt{3} & 1/\sqrt{3} \\ 1/\sqrt{2} & -1/\sqrt{2} & 0 \\ 1/\sqrt{6} & -1/\sqrt{6} & -2/\sqrt{6} \end{bmatrix}, \tag{2}$$

while $\mathbb{I}_3$, and $\mathbb{O}_3$ are, respectively, the 3×3 identity and zeros matrices. Here, as usual, e_1 is the hydrostatic strain, e_2 and e_3 are deviatoric strains, and e_4, e_5, e_6 are shear strains. The deviatoric strains are chosen as order parameters to describe different phases in the domain. The free-energy functional $\mathscr{F}$ for the cubic-to-tetragonal phase transformation can be written as [**?**], [8]:

$$\mathscr{F}[\boldsymbol{u}] = \int_\Omega \left[F_0(e_1, \ldots, e_6, \theta) + \frac{k_g}{2} \left(|\nabla e_2|^2 + |\nabla e_3|^2 \right) \right] \mathrm{d}\Omega, \tag{3}$$

where

$$F_0(e_1, \ldots, e_6, \theta) = \frac{a_1}{2} e_1^2 + \frac{a_2}{2} \left(e_4^2 + e_5^2 + e_6^2 \right) + a_3 \tau \left(e_2^2 + e_3^2 \right) + a_4 e_3 \left(e_3^2 - 3e_2^2 \right) + a_5 (e_2^2 + e_3^2)^2. \tag{4}$$

In (3)–(4) a_i, $i \in \{1, \ldots, 5\}$ are constants that define the mechanical properties of the material, k_g is the gradient energy coefficient, $\tau = (\theta - \theta_m)/(\theta_0 - \theta_m)$ is the dimensionless temperature, where θ_0 and θ_m are the material properties specifying the transformation start temperature and the temperature at which austenite becomes unstable, and $|\cdot|$ denotes the Euclidean norm of a vector. By using these notations, the core part of the model of interest in this paper can be given as

$$\rho \ddot{u}_i = \sigma_{ij,j} + \eta \sigma'_{ij,j} + \mu_{ij,kkj} + f_i, \tag{5}$$

$$C_v \dot{\theta} = \kappa \theta_{,ii} + \Xi \theta \left(u_{i,i} \dot{u}_{j,j} - 3u_{i,i} \dot{u}_{i,i} \right) + g, \tag{6}$$

where ρ, η, C_v, κ, and Ξ represent the density, viscous dissipation, specific heat, thermal conductance coefficient, and strength of the thermo-mechanical coupling, respectively (they are all positive constants). To give a flavor of the complexity of the non-linear model we are dealing with here, we provide explicit expressions for the symmetric stress tensor $\boldsymbol{\sigma} = \{\sigma_{ij}\}$ components which are strongly nonlinear functions of e_i, as well as the temperature:

$$\sigma_{11} = \frac{a_1 e_1}{\sqrt{3}} + \frac{e_2}{\sqrt{2}} \left[2\tau a_3 - 6a_4 e_3 + 4a_5 (e_2^2 + e_3^2) \right] + \frac{1}{\sqrt{6}} \left[e_3 (2\tau a_3 + 4a_5 (e_2^2 + e_3^2)) + 3a_4 (e_3^2 - e_2^2) \right], \tag{7.1}$$

$$\sigma_{12} = \sigma_{21} = \frac{1}{2} a_2 e_6, \tag{7.2}$$

$$\sigma_{13} = \sigma_{31} = \frac{1}{2} a_2 e_5, \tag{7.3}$$

$$\sigma_{22} = \frac{a_1 e_1}{\sqrt{3}} - \frac{e_2}{\sqrt{2}} \left[2\tau a_3 - 6a_4 e_3 + 4a_5 (e_2^2 + e_3^2) \right] + \frac{1}{\sqrt{6}} \left[e_3 (2\tau a_3 + 4a_5 (e_2^2 + e_3^2)) + 3a_4 (e_3^2 - e_2^2) \right], \tag{7.4}$$

$$\sigma_{23} = \sigma_{32} = \frac{1}{2} a_2 e_4, \tag{7.5}$$

$$\sigma_{33} = \frac{1}{\sqrt{3}} a_1 e_1 - \frac{2}{\sqrt{6}} \left[2\tau a_3 e_3 + 3a_4 (e_3^2 - e_2^2) + 4a_5 e_3 (e_2^2 + e_3^2) \right]. \tag{7.6}$$

The only thing left to be explained in the above model is the dissipational stress tensor, $\boldsymbol{\sigma}' = \{\sigma'_{ij}\}$. It is a linear function of the strain rates $\dot{e}_i$, $i = 1, \ldots, 6$. More precisely, $\boldsymbol{\sigma}'$ is a second-rank symmetric tensor, hence only six entries are required for its definition:

$$\begin{Bmatrix} \sigma'_{11} \\ \sigma'_{22} \\ \sigma'_{33} \\ \sigma'_{23} \\ \sigma'_{13} \\ \sigma'_{12} \end{Bmatrix} = \left[\begin{array}{c|c} \mathbb{D}_3^T & \mathbb{O}_3 \\ \hline \mathbb{O}_3 & \frac{1}{2}\mathbb{I}_3 \end{array}\right] \begin{Bmatrix} \dot{e}_1 \\ \dot{e}_2 \\ \dot{e}_3 \\ \dot{e}_4 \\ \dot{e}_5 \\ \dot{e}_6 \end{Bmatrix}. \tag{8}$$

Note also that the microstress tensor, $\boldsymbol{\mu} = \{\mu_{ij}\} = \frac{k_g}{3}\left(\nabla^T \boldsymbol{u} - 3\nabla_d \boldsymbol{u}\right)$, is the second-rank tensor which is non-symmetric.

$\boldsymbol{\mu} =$, where $\nabla^T \boldsymbol{u}$ is the transpose of the displacement gradient (i.e., $\nabla^T \boldsymbol{u} = \{u_{j,i}\}$), and $\nabla_d \boldsymbol{u} = \mathrm{diag}(u_{1,1}, u_{2,2}, u_{3,3})$ with $\mathrm{diag}(a, b, c)$. Right hand side parts in our equations ($\boldsymbol{f} = \{f_1, f_2, f_3\}^T$ and g) represent mechanical and thermal loads.

A. Complete Model in a Strong Form

We complete the formulation of the model by adding appropriate boundary and initial conditions. In particular, for the temperature we have

$$\theta_{,i} n_i = 0, \qquad \text{on } \Gamma \times (0, T), \tag{9}$$

whereΓ is the boundary of Ω, and its outward normal has been denoted heere by $\boldsymbol{n}$. These are typical insulated boundary conditions on Γ for the temporal interval of interest $(0, T)$.

For the displacement field we need two boundary conditions The first boundary condition is imposed on the entire boundary. Namely, the normal component of the gradient of the microstress tensor vanishes:

$$\mu_{ij,k} n_k = 0, \qquad \text{on } \Gamma \times (0, T). \tag{10}$$

For the remaining boundary condition we consider either imposed displacements or stress-free conditions. For a formal formulation, one can assume that Γ admits decompositions:

$$\left.\begin{array}{rcl} \Gamma & = & \overline{\Gamma_{Di} \cup \Gamma_{Si}} \\ \emptyset & = & \Gamma_{Di} \cap \Gamma_{Si} \end{array}\right\}; \; i = 1, 2, 3. \tag{11}$$

This allows to formulate mechanical boundary for each spatial direction i as follows:

$$\begin{aligned} \left(\sigma_{ij} + \eta\sigma'_{ij} + \Delta\mu_{ij}\right) n_j &= 0, \qquad \text{on} \quad \Gamma_{Si} \times (0, T), && (12) \\ u_i &= u_i^D, \qquad \text{on} \quad \Gamma_{Di} \times (0, T), && (13) \end{aligned}$$

where u_i^D's are known functions, prescribing the displacements on the corresponding parts of the boundary.

As a result, the complete problem to be solved can be formulated as follows:

$$\begin{aligned}
&\rho\ddot{u}_i = \sigma_{ij,j} + \eta\sigma'_{ij,j} + \mu_{ij,kkj} + f_i, && \text{in } \Omega \times (0, T), && (14.1) \\
&C_v\dot{\theta} = \kappa\theta_{,ii} + \Xi\theta\left(u_{i,i}\dot{u}_{j,j} - 3u_{i,i}\dot{u}_{i,i}\right) + g, && \text{in } \Omega \times (0, T), && (14.2) \\
&\mu_{ij,k} n_k = 0, && \text{on } \Gamma \times (0, T), && (14.3) \\
&\left(\sigma_{ij} + \eta\sigma'_{ij} + \Delta\mu_{ij}\right) n_j = 0, && \text{on } \Gamma_{Si} \times (0, T), && (14.4) \\
&u_i = u_i^D, && \text{on } \Gamma_{Di} \times (0, T), && (14.5) \\
&\theta_{,i} n_i = 0, && \text{on } \Gamma \times (0, T), && (14.6) \\
&u_i(\boldsymbol{x}, 0) = u_i^0(\boldsymbol{x}), && \text{in } \overline{\Omega}, && (14.7) \\
&\theta(\boldsymbol{x}, 0) = \theta^0(\boldsymbol{x}), && \text{in } \overline{\Omega}, && (14.8)
\end{aligned}$$

where $u_i^0 : \overline{\Omega} \mapsto \mathbb{R}$, $\theta_0 : \overline{\Omega} \mapsto \mathbb{R}$ are known functions defining the displacements and temperature in the closed domain $\overline{\Omega}$ at the initial moment of time. From a mechanics point of view, it is strongly non-linear of coupled dynamic thermoelasticity.

III. WEAK FORM AND IGA-BASED NUMERICAL FORMULATION

Before we turn to the main result of numerical simulations obtained from this model by using the isogeometric analysis, we note that the entire computational domain was discretized with $\mathscr{C}^1$-continuous functions (to deal with fourth-order PDEs). The integration in time was carried out with the generalized-α method.

Spatial discretization of the problem (14) was based on its re-formulation in a weak form. First, we defined the trial solution spaces

$$\mathcal{S}_i = \left\{u_i \in \mathcal{H}^2 \mid u_i = u_i^D \text{ on } \Gamma_{Di}\right\},\ i = 1, 2, 3, \quad (15)$$

$$\mathcal{S}_\theta = \left\{\theta \in \mathcal{H}^1\right\}, \quad (16)$$

as well as the spaces:

$$\mathcal{W}_i = \left\{w_i \in \mathcal{H}^2 \mid w_i = 0 \text{ on } \Gamma_{Di}\right\},\ i = 1, 2, 3, \quad (17)$$

$$\mathcal{W}_q = \left\{q \in \mathcal{H}^1\right\}. \quad (18)$$

where $\mathcal{H}^k$ is the Sobolev space of square-integrable functions with square-integrable derivatives up to order k. To derive the weak formulation we follow a standard methodology. In our case, we multiply the mechanical part equations by w_i and integrate the result by parts several times. As for the thermal part equation, we multiply it by q and integrate the result by parts once. The weak (variational) formulation of our problem can then be presented as follows. We seek $\mathsf{S} = \{\boldsymbol{u}, \theta\} \in \mathcal{S}_1 \times \mathcal{S}_2 \times \mathcal{S}_3 \times \mathcal{S}_\theta$ such that $\mathsf{B}(\mathsf{S}, \mathsf{W}) = 0$ for all $\mathsf{W} = \{\boldsymbol{w}, \theta\} \in \mathcal{W}_1 \times \mathcal{W}_2 \times \mathcal{W}_3 \times \mathcal{W}_\theta$, where

$$\begin{aligned}\mathsf{B}(\mathsf{S}, \mathsf{W}) = \quad & (w_i, (\rho \ddot{u}_i - f_i)) + \left(w_{i,j}, \sigma_{ij} + \eta \sigma'_{ij}\right) - (w_{i,jk}, \mu_{ij,k}) \\ + \quad & \left(q, \left(C_v \dot{\theta} - \Xi \theta (u_{i,i} \dot{u}_{j,j} - 3u_{i,i} \dot{u}_{i,i}) - g\right)\right) + (\kappa q_{,i}, \theta_{,i}). \end{aligned} \quad (19)$$

IV. COMPUTATIONAL EXPERIMENTS

Our results concern with the microstructure evolution and its effect on thermo-mechanical properties of SMA specimens. It is one of the key issues in further improvements of SMA-based devices and systems for structural control and monitoring.

The model (its strong formulation (14)) was rescaled and converted into the weak formulation, according to the procedure highlighted above. In obtaining numerical results reported here, we have used $Fe_{70}Pd_{30}$ SMA samples. Their material parameters are summarized in Table I (see also [8]). Our computational domains in all cases have been discretized by using B-spline or NURBS basis functions with $\mathscr{C}^k$ global continuity for $k \geq 1$.

TABLE I

$Fe_{70}Pd_{30}$ MATERIAL CONSTANTS

a_1	a_2	a_3	a_4	a_5	η
192.3 GPa	280 GPa	19.7 GPa	2.59 × 10^3 GPa	8.52 × 10^4 Gpa	0.25 N-s m^2
k_g	θ_m	θ_0	C_v	κ	ρ
3.15 × 10^{-8} N	270 K	295 K	350 J kg^{-1} K^{-1}	78 W m^{-1} K^{-1}	10000 kg m^{-3}

We note that the spatial mesh in all computations has been refined by using the classical h-refinement and the new paradigm for mesh refinement introduced by IGA, k-refinement, in which the order of the basis functions is elevated, with their global continuity increased. We carried out numerical simulations of dynamic SMAs for various geometries, including cubic, slab, cylindrical, tubular torus, and others. In what follows, we present results for SMA nanofilms.

Nanostructured thin-film SMAs have been subjected to stress-induced loadings due to pre-stretching. The 150x150x5 nm thin-film has been meshed with a 120x120x4 $\mathscr{C}^1$-continuous quadratic B-spline. The pre-stretching has been achieved by loading the thin-film boundaries with prescribed non-zero displacement $u_1 = u_2 = \bar{u} =$ 3.75 nm and u_3 = 0 nm at t = 0 ns, along the out-of-material normal direction as shown in Fig. 1(a). The initial temperature of the thin-film was set 240 K. The periodic boundary conditions for displacements were applied on the SMA thin-film along the x_3 direction.

The microstructure morphology at different time instants are shown in Figs. 1(b–f). The M_1, M_2, and M_3 martensitic variants are represented in red, blue, and green colors, respectively. It can be clearly seen that the microstructures start to nucleate, evolve and self-accommodate. Due to the prescribed non-zero displacements at the thin-film boundaries, the domain walls between variants do no adhere along [110] planes. The microstructures coalease to form different martensitic variants pockets as shown in Fig. 1(f). The results suggest that the geometry and boundary conditions can be used to alter the domain wall directions.

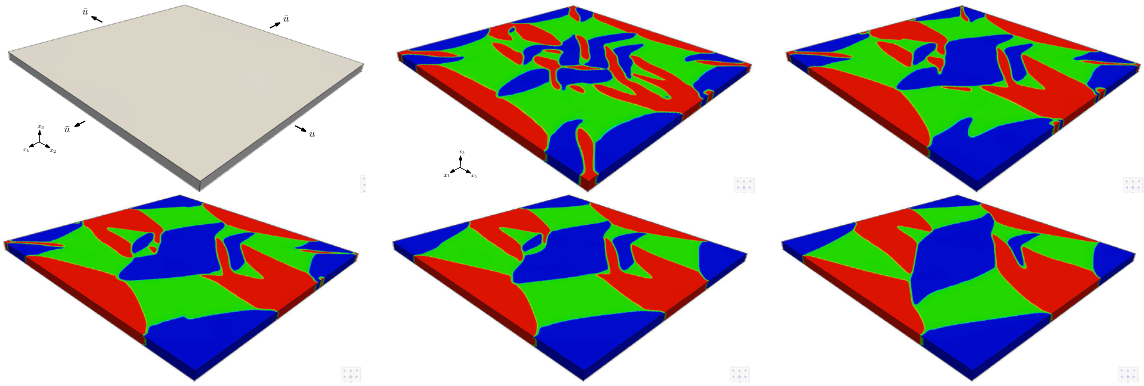

Fig. 1. (Color online) From left-to-right in the upper and then lower panels: (a) Schematic loading, (b) $t = 0.09\text{ns}$, (c) $t = 0.18\text{ns}$, (d) $t = 0.27\text{ns}$, (e) $t = 0.36\text{ns}$, (f) $t = 1.08\text{ns}$. Self-accommodated microstructure in pre-stretched 150x150x5 nm thin-film (red, blue, and green colors represent M_1, M_2, and M_3 variants, respectively).

V. CONCLUSIONS

A 3D phase-field coupled dynamic model for cubic-to-tetragonal phase transformations has been presented to study complex thermo-mechanical behavior of SMAs. The model has been numerically implemented in the IGA framework and advantages of such an implementation have been highlighted. The results of simulations, exemplified for SMA thin films, have demonstrated the influence of microstructure evolution thermo-mechanical properties of SMA specimens. They can provide guidelines for further improvements of SMA-based devices and systems for structural control and monitoring.

ACKNOWLEDGMENT

RD, RM, and JZ have been supported by the NSERC and CRC program (RM), Canada. RM and AS acknowledge the TUBITAK support. HG was partially supported by the European Research Council through the FP7 Ideas Starting Grant program (project # 307201) and by *Consellería de Educación e Ordenación Universitaria* (*Xunta de Galicia*). Their support is gratefully acknowledged. This work was made possible with the facilities of the Shared Hierarchical Academic Research Computing Network (SHARCNET: www.sharcnet.ca) and Compute/Calcul Canada.

REFERENCES

[1] K. Bhttacharya, R. James, ”The material is the machine”, *Science*, vol. 307 (5706), pp. 53–54, 2005.
[2] R. V. N. Melnik, A. J. Roberts, and K. A. Thomas, ”Computing Dynamics of Copper-Based SMA via Centre Manifold Reduction of 3D Models”, *Computational Materials Science*, vol. 18, pp. 255–268, 2000.
[3] R. Dhote, H. Gomez, R. Melni, and J. Zu, ”Isogeometric analysis of a dynamic thermo-mechanical phase-field model applied to shape memory alloys”, *Computational Mechanics*, doi: 10.1007/s00466-013-0966-0, 2014.
[4] D. Konig, M. Ehmann, S. Thienhaus, A. Ludwig, ”Micro-to nanostrcuctured devices for the characterization of scaling effects in shape-memory thin films”, *Journal of Microelectromechanical Systems*, vol. 19 (5), pp. 1264–1269, 2010.
[5] B. Bayer, S. Sanjabi, C. Baehtz, C. Wirth, S. Esconjauregui, R. Weatherup, Z. Barber, S. Hofmann, J. Robertson, ”Carbon nanotubeforest growth on NiTi shape memory alloy thin films for thermal actuation”, *Thin Solid Films*, vol. 519 (18), pp. 6126–6129, 2011.
[6] R. Dhote, H. Gomez, R. Melni, and J. Zu, ”Isogeometric analysis of coupled thermo-mechanical phase-field models using distributed computing”, *Procedia Computer Science*, vol. 18, pp. 1068–1076, 2013.
[7] R. Dhote, H. Gomez, R. Melni, and J. Zu, ”3D coupled thermo-mechanical phase-field modeling of shape memorry alloy dynamics via isogeometric analysis”, Computer Methods in Applied Mechanics and Engineering, submitted for publication.
[8] R. Ahluwalia, T. Lookman, A. Saxena, ”Dynamic strain loading of cubic to tetragonal martensites”, *Acta Materialia*, vol. 54, pp. 2109–2120, 2006.

CIMNE
International Center
for Numerical Methods in Engineering

UNIVERSITAT POLITÈCNICA
DE CATALUNYA
BARCELONATECH

EACS

CoDAlab
Control, Dynamics and Applications
Matemàtica Aplicada III - Universitat Politècnica de Catalunya

IASCM

IK4 IKERLAN
Research Alliance

Centro tecnológico
CARTIF

Smart Materials and Structures

WILEY

Fiber Sensing


6WCSCM
Sixth World Conference on
Structural Control and Monitoring
Barcelona, Spain, 15 - 17 July 2014
J. Rodellar, A. Güemes and F. Pozo (Eds.)
CIMNE
Deposito Legal: B-16310-2014
ISBN: 978-84-942844-5-8
ebook by CIMNE